Chinese Journal of Natural Medicines

Comprehensive analysis of the antibacterial activity of 5,8-dihydroxy-1,4-naphthoquinone derivatives against methicillin-resistant *Staphylococcus aureus*

Qingqing Chen, Yuhang Ding, Zhongyi Li, Xingyu Chen, Aliya Fazal, Yahan Zhang, Yudi Ma, Changyi Wang, Liu Yang, Tongming Yin, Guihua Lu, Hongyan Lin, Zhongling Wen, Jinliang Qi, Hongwei Han, Yonghua Yang

Citation: Qingqing Chen, Yuhang Ding, Zhongyi Li, Xingyu Chen, Aliya Fazal, Yahan Zhang, Yudi Ma, Changyi Wang, Liu Yang, Tongming Yin, Guihua Lu, Hongyan Lin, Zhongling Wen, Jinliang Qi, Hongwei Han, Yonghua Yang, Comprehensive analysis of the antibacterial activity of 5,8-dihydroxy-1,4-naphthoquinone derivatives against methicillin-resistant *Staphylococcus aureus*, Chinese Journal of Natural Medicines, 2025, 23(5), 604-613. doi: 10.1016/S1875-5364(25)60818-1.

View online: https://doi.org/10.1016/S1875-5364(25)60818-1

Chinese Journal of Natural Medicines 23 (2025) 604-613

Contents lists available at ScienceDirect

Chinese Journal of Natural Medicines

journal homepage: www.cjnmcpu.com/

Original article

Comprehensive analysis of the antibacterial activity of 5,8-dihydroxy-1,4-naphthoquinone derivatives against methicillin-resistant *Staphylococcus aureus*

Qingqing Chen[a,b], Yuhang Ding[a,b], Zhongyi Li[a,b], Xingyu Chen[a], Aliya Fazal[a,b], Yahan Zhang[a], Yudi Ma[a], Changyi Wang[a], Liu Yang[a], Tongming Yin[b], Guihua Lu[a,b], Hongyan Lin[a,b,c], Zhongling Wen[a,b,*], Jinliang Qi[a,b,*], Hongwei Han[a,b,*], Yonghua Yang[a,b,*]

[a] *State Key Laboratory of Pharmaceutical Biotechnology, Institute of Plant Molecular Biology, School of Life Sciences, Nanjing University, Nanjing 210023, China*
[b] *Co-Innovation Center for Sustainable Forestry in Southern China, Nanjing Forestry University, Nanjing 210037, China*
[c] *School of Pharmacy, Changzhou University, Changzhou 213164, China*

ARTICLE INFO

Article history:
Received 2 October 2024
Revised 1 December 2024
Accepted 5 January 2025
Available online 20 May 2025

Keywords:
5,8-Dihydroxy-1,4-naphthoquinone
Antibacterial activity
MRSA
Arginine biosynthesis
Pyrimidine metabolism

ABSTRACT

Given the increasing concern regarding antibacterial resistance, the antimicrobial properties of naphthoquinones have recently attracted significant attention. While 1,4-naphthoquinone and its derivatives have been extensively studied, the antibacterial properties of 5,8-dihydroxy-1,4-naphthoquinone derivatives remain relatively unexplored. This study presents a comprehensive *in vitro* and *in vivo* analysis of the antibacterial activity of 35 naturally sourced and chemically synthesized derivatives of 5,8-dihydroxy-1,4-naphthoquinone. Kirby-Bauer antibiotic testing identified three compounds with activity against methicillin-resistant *Staphylococcus aureus* (MRSA), with one compound (PNP-02) demonstrating activity comparable to vancomycin in minimum inhibitory concentration, minimum bactericidal concentration (MBC), and time-kill assays. Microscopic and biochemical analyses revealed that PNP-02 adversely affects the cell wall and cell membrane of MRSA. Mechanistic investigations, including proteomic sequencing analyses, Western blotting, and RT-qPCR assays, indicated that PNP-02 compromises cell membrane integrity by inhibiting arginine biosynthesis and pyrimidine metabolism pathways, thereby increasing membrane permeability and inducing bacterial death. In an *in vivo* mouse model of skin wound healing, PNP-02 exhibited antibacterial efficacy similar to vancomycin. The compound demonstrated low toxicity to cultured human cells and in hemolysis assays and remained stable during serum incubation. These findings suggest that PNP-02 possesses promising bioactivity against MRSA and represents a potential novel antibacterial agent.

1. Introduction

Staphylococcus aureus, a Gram-positive bacterium, is responsible for various infections in humans and animals, ranging from cutaneous manifestations to severe systemic conditions such as sepsis and meningitis [1, 2]. The indiscriminate use of antibiotics has precipitated the emergence of drug-resistant bacterial strains, presenting a significant challenge to both human and animal health [3-6]. Of particular concern is the escalating public health threat posed by multidrug-resistant *S. aureus* strains, notably methicillin-resistant *S. aureus* (MRSA). This strain has been associated with a mortality rate surpassing that of AIDS, tuberculosis, and viral hepatitis combined [7]. Accordingly, the quest for innovative and structurally diverse compounds that exhibit potential antimicrobial properties is increasingly important in the face of rising antibiotic resistance.

Natural products have been a crucial source of antibacterial medications for centuries, prized for their biocompatibility and efficacy [6]. Naphthoquinones, a class of natural compounds, have gained recognition for their diverse clinical applications, including antibacterial, antitumor, and antioxidant properties, primarily due to their unique redox characteristics [8]. Both naturally occurring and synthetic derivatives of 1,4-naphthoquinone demonstrate potent effects against various conditions, exhibiting strong anti-malarial, antitumor, anti-inflammatory, antifungal, and antibacterial properties [9, 10]. In traditional medicine, 1,4-naphthoquinone, 2-amino-1,4-naphthoquinone, and lawsone have established roles as effective anticancer, anti-malarial, and antibacterial agents [11]. Research has shown that 1,4-naphthoquinone exerts antimicrobial effects against S. aureus by promoting the accumulation of reactive oxygen species (ROS) within bacterial cells [12].

Despite these promising findings, there is still a lack of research focused on elucidating the antibacterial mechanisms associated with naphthoquinones. These effects have been primarily

* Corresponding author.
E-mail addresses: wenzhongling@nju.edu.cn (Z. Wen); qijl@nju.edu.cn (J. Qi); hanhw18@nju.edu.cn (H. Han); yangyh@nju.edu.cn (Y. Yang)

https://doi.org/10.1016/S1875-5364(25)60818-1

attributed to the inhibition of electron transfer within the mitochondrial respiratory chain, leading to increased production of ROS and radical semiquinones [13, 14]. A study by Duvauchelle *et al.* [8] examined the antibacterial potential of 29 derivatives of juglone and 1,4-naphthoquinone against both reference strains and clinical isolates of Gram-positive and Gram-negative bacteria. Their findings revealed that the synthesized juglone/naphthazarin derivatives demonstrate considerable antibacterial activity, particularly against clinically resistant strains of *S. aureus*, indicating their potential for further development in therapeutic applications. However, *in vitro* and *in vivo* experiments designed to investigate the underlying mechanisms of action of these derivatives against MRSA remain scarce.

One derivative, 5,8-dihydroxy-1,4-naphthoquinone, was demonstrated by Topçu et al. to eliminate a range of bacteria and fungi, including *S. aureus* and *Candida albicans*, by disrupting their cell membranes. This compound has been recognized as a potent antifungal and antibacterial substance, establishing a firm basis for ongoing research and development [14, 15]. Although the antibacterial properties of 5,8-dihydroxy-1,4-naphthoquinone have been reported, its influence on MRSA infections has not been well explored. Moreover, there exists a lack of studies concentrating on the antibacterial actions and mechanisms of 5,8-dihydroxy-1,4-naphthoquinone and its related compounds.

Shikonin, a compound derived from 5,8-dihydroxy-1,4-naphthoquinone, demonstrates diverse therapeutic properties, including antibacterial, antitumor, anti-inflammatory, and wound healing promotion effects [16]. Research by Li et al. revealed that combining shikonin with conventional antibiotics produces a synergistic anti-MRSA activity, potentially attributable to the suppression of penicillin-binding protein 2a expression and compromised membrane function [17].

Previously, our laboratory synthesized various shikonin derivatives and observed antitumor effects in several compounds (Table 1). However, their antibacterial properties and underlying molecular mechanisms remained unexplored. This study evaluated the antimicrobial activity of 10 available natural 5,8-dihydroxy-1,4-naphthoquinone derivatives alongside 25 naphthoquinone derivatives selected from 389 compounds synthesized in our laboratory. We conducted a comprehensive, systematic examination of the antibacterial activities and mechanisms of action of these naphthoquinone derivatives against MRSA (Fig. 1).

2. Material and methods

2.1. Bacterial strains and growth conditions

S. aureus USA300, *Bacillus subtilis,* and *Escherichia coli* were obtained from the State Key Laboratory of Medical Biotechnology at Nanjing University. MRSA ATCC 43300 was sourced from the Guangdong Microbial Species Preservation Center. All strains were cultured overnight in Mueller-Hinton (MH) medium at 37 °C. Bacterial suspensions with a density of 1×10^6 CFU/mL were prepared for subsequent experiments.

2.2. Antimicrobial agents and chemicals

Nine natural 5,8-dihydroxy-1,4-naphthoquinone derivatives (purity > 98%) were purchased from Shanghai Yuanye Biotechnology Co., Ltd. Shikonin, and 25 5,8-dihydroxy-1,4-naphthoquinone derivatives (purity > 98%) were obtained from our laboratory. Vancomycin and penicillin were purchased from Solarbio Technology Co., Ltd. (Beijing, China). Stock solutions of all compounds were prepared at a concentration of 1280 μg·mL^{-1} in dimethyl sulfoxide (DMSO) or double-distilled H_2O. Fetal bovine serum was purchased from Wuhan Sunncell Biotechnology Co., Ltd. Biochemical kits to determine the activities of lactate dehydrogenase (LDH) and alkaline phosphatase (ALP) were purchased from Biyuntian Biotechnology Co., Ltd. (Shanghai, China).

2.3. Antimicrobial susceptibility test

The antimicrobial susceptibility of MRSA strains was assessed using the Kirby-Bauer disk diffusion method [18].

The minimum inhibitory concentration (MIC) of each antimicrobial was determined by microdilution according to Clinical and Laboratory Standards Institute (CLSI) guidelines [19]. Specifically, bacterial viability was assessed using 0.1% (*W/V*) resazurin (Coolaber, Beijing, China). The MIC was defined as the lowest concentration of 5,8-dihydroxy-1,4-naphthoquinone derivatives that inhibited bacterial growth. The minimum bactericidal concentration (MBC) was determined by removing 100 μL from each well without visible bacterial growth, subculturing on agar plates, and incubating at 37 °C for 24 h [20].

2.4. Time-kill assay

Time-kill assays were conducted to evaluate the bactericidal efficacy of SK derivatives against MRSA, following previously established protocols [21]. The bactericidal effect was assessed by combining MRSA strains (1×10^6 to 1×10^7 CFU·mL^{-1}) with varying concentrations of PNP-02 (0, 1, 2, 4, and 8 μg·mL^{-1}) in PBS. The mixtures were agitated at 240 r·min^{-1} for 4 h at 37 °C. Subsequently, 0.1 mL of the bacterial suspensions were plated on MH agar and incubated for 12 h at 37 °C, after which colony counts were performed. To generate time-kill curves, samples from the PNP-02-treated bacterial suspensions were also collected at 0, 1, 2, 4, 6, and 8 h intervals.

2.5. Crystal violet assay

PNP-02 was added to MRSA cultures growing in the MH medium, and the mixture was subsequently transferred to 96-well plates. The final bacterial concentration in each well was maintained at 1×10^7 CFU·mL^{-1}, while PNP-02 concentrations were set at 0.5 ×, 1 ×, and 2 × MIC. The 96-well plates were then incubated at 37 °C for 24 h. Biofilm formation was quantified using the crystal violet assay, as described in previous literature [22].

2.6. Transmission electron microscopy (TEM)

The impact of PNP-02 on the MRSA cell membrane was investigated using TEM as previously described [23]. MRSA cells (1×10^8 CFU·mL^{-1}) were exposed for 2 h to PNP-02 at concentrations equivalent to 1 × or 2 × MIC. The untreated (control) and treated cells were washed and collected, followed by a 12-h fixation with 2.5% glutaraldehyde in PBS at 4 °C. Fixed cells were washed twice and post-fixed with 1% osmium tetroxide in 1 × PBS. Subsequently, the cells were washed in PBS and dehydrated in ethanol, propylene oxide, and serial solutions of acetone. Polymerized specimen blocks were sectioned into 1 μm-thick slices, and specimens were double stained with uranyl acetate followed by lead citrate. The samples were then examined using a Hitachi H-7650 transmission electron microscope (Camera: GatanErlangshen ES500W, Peabody, MA, USA) at an accelerating voltage of 100 kV.

2.7. Propidium iodide (PI) staining assay

The effect of PNP-02 on MRSA cell membranes was investigated using a PI staining assay, following the established described [24]. Bacterial cells were incubated with PNP-02 at concentrations of 0.5 ×, 1 ×, and 2 × MIC for 1 h. After removing the supernatant, the cells were washed with 3 mL PBS and resuspen-

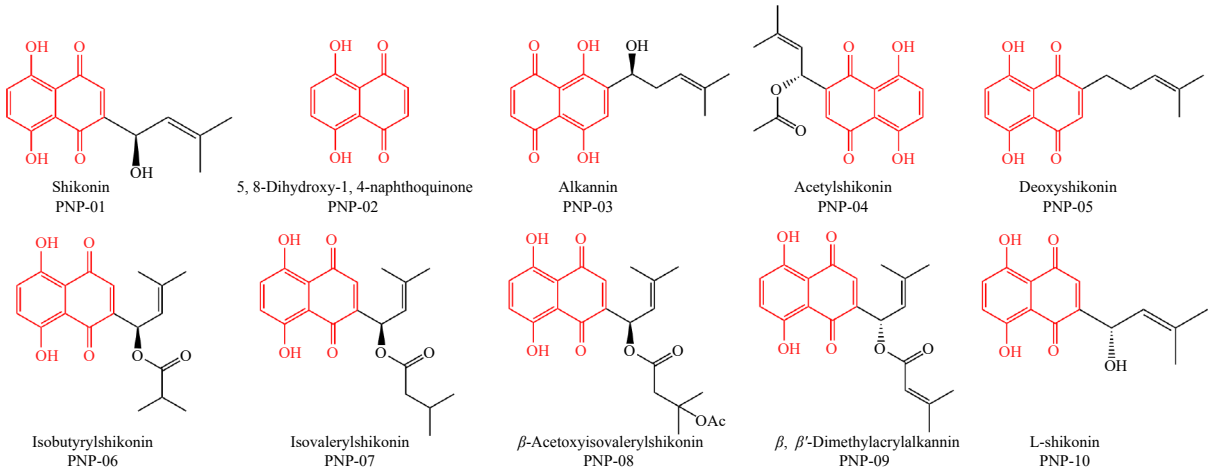

Fig. 1 Chemical structures of the 10 natural naphthoquinone derivatives.

ded in PBS to achieve a bacterial density of approximately 10^6 CFU. The bacteria were stained by incubation in the dark. Subsequently, the supernatant was removed, and the cells were washed three times with PBS and resuspended in 200 μL PBS. The numbers of PI-stained cells were determined using fluorescence microscopy.

2.8. Measurement of the leakage of intracellular contents

The effect of PNP-02 on the structural integrity of MRSA cells was examined by measuring the release of LDH and ALP into the culture media, following the established method [25]. Briefly, bacterial strains were exposed to PNP-02 at concentrations of 0, 1, 2, and 4 μg·mL^{-1} for 0, 2, 4, or 6 h. Subsequently, bacterial cells were collected for LDH level measurement, while supernatants were obtained to assess ALP activity. Enzyme activities were quantified using specialized biochemical assay kits.

2.9. Hemolysis assay

The assessment of goat red blood cell hemolysis was conducted following the method described by Duan *et al.* [26] Goat erythrocytes (5%) were exposed to PNP-02 at concentrations ranging from 0.25 to 32 μg·mL^{-1} for 1 h. Subsequently, each mixture underwent centrifugation at 3000 g for 15 minutes to separate intact red blood cell granules. The supernatants' absorbance was measured at 540 nm using a spectrophotometer. Saline served as the negative control, while 1% Triton X-100 was employed as the positive control. The hemolysis ratio was determined using equation (1).

$$Hemolysis(\%) = \frac{OD_{540}(PNP-02) - OD_{540}(saline)}{OD_{540}(TritonX100) - OD_{540}(saline)} \times 100 \quad (1)$$

2.10. Cell Counting Kit-8 (CCK-8) assay

LO2 cells were seeded into 96-well plates and then incubated with PNP-02 at 37 °C for 24 h. CCK-8 solution was added, and the cells were incubated for an additional 2 h. The absorbance at 450 nm was measured using a microplate reader (ELx800, BioTek, USA).

2.11. Plasma stability assay

Sterile sheep blood was centrifuged at 4000 r·min^{-1} for 10 min, and the supernatant was harvested as freshly prepared plasma [27]. Solutions containing 50% plasma were combined with PNP-02 in 96-well plates, and these samples were incubated at 37 °C for 0, 3, or 6 hours. Following the incubation, aliquots (150 μL) of an MRSA suspension were added, and the plates were further incubated at 37 °C for 16 to 24 h. The stability of compound PNP-02 in plasma was assessed by determining the MBC as outlined in section 2.3.

2.12. Proteomic and bioinformatic analyses

Proteome sequencing was conducted utilizing the TMT-labeled quantitative proteomics technique [28]. The proteomic analysis was performed by Luming Technology Co., Ltd. (Shanghai, China). Samples underwent reduction, alkylation, and trypsin digestion for 20 h at 37 °C to release peptides. The resulting peptide mixtures were separated and analyzed using the EASY-nLC™ 1000 chromatography system coupled to a Q-Exactive HF hybrid quadrupole-orbitrap mass spectrometer (Thermo, USA). The LC-MS/MS raw data were processed using MaxQuant software for analysis. The false-positive rate for peptide identification was maintained below 1%.

The Gene Ontology (GO, https://geneontology.org/), Uniprot, LOG/COG, and String (https://string-db.org/) databases were used to investigate the biological functions and physical and chemical properties of proteins bound to PNP-02. The information obtained included the protein class, cellular component, biological process, and molecular function, as well as the corresponding molecular weight. The Kyoto Encyclopedia of Genes and Genomes (KEGG) resource was used for pathway analyses.

2.13. Reverse transcription-quantitative polymerase chain reaction (RT-qPCR)

To validate the proteomic data, we selected several genes that were downregulated following PNP-02 treatment and assessed the relative expression levels of these genes by real-time RT-qPCR [29, 30]. The extraction of total RNA was performed using the E.Z.N.A.® bacterial RNA kit (TIANGEN, China). The mRNA was reverse transcribed into cDNA using the QuantiTect reverse transcription kit (TIANGEN, Beijing, China). RT-qPCR was conducted using the StepOnePlus real-time PCR system. The relevant primers and genes are listed in Table S1.

2.14. Western blotting

Western blotting assays were performed as previously described [31]. MRSA was cultured in MH medium and subsequently exposed to PNP-02 at concentrations of 0.5 ×, 1 ×, or 2 × MIC for 24 h. Bacterial cells were harvested by centrifugation at 13 000 r·min^{-1} for 10 min. The cell lysates were mixed with a non-redu-

cing channel-labeled sample buffer and subjected to heat denaturation. The proteins were separated using 10% SDS-PAGE and transferred to polyvinylidene fluoride blotting membranes. The membranes were blocked, and antibodies were applied using standard techniques. Detection was performed by enhanced chemiluminescence reagent (Thermo Fisher Scientific, USA) according to the manufacturer's instructions. The resulting bands were visualized using a gel imaging system, and the data were analyzed using ImageJ software.

2.15. Mouse skin wound healing assay

Animal experimental protocols were approved by the Animal Ethics Committee at Huachuang Sino, Taizhou, China (Approval No. SY23033-P001-01). A total of forty female CD1 ICR outbred mice aged 8 weeks and weighing between 18–20 g (Certification: SYXK(Su)2020-0041) were procured from Jiangsu Huachuang Sino Pharma Tech Co., Ltd. (Nanjing, China). The mice underwent a one-week adaptive feeding period before the commencement of experiments. Throughout the study, all mice had unrestricted access to water and food.

All mice were anesthetized using a 10% chloral hydrate solution to ensure they remained unresponsive during the procedure. Subsequently, a precise 1-centimeter incision was made on the dorsal skin of each mouse, extending to the dermal layer to facilitate the required experimental observations and interventions [24]. Following randomization, participants were allocated to one of five groups: control, model, 0.5 × MIC PNP-02, 1 × MIC PNP-02, and 2 × MIC PNP-02. Each group comprised five mice. The incisions were inoculated with 200 μL of MRSA isolate solution (1×10^8 CFU/mL). At 24 h post-inoculation, 100 μL of PBS and varying concentrations of PNP-02 were applied to the infection site four times within 1 h, respectively. Mice received treatment every 24 h. The incisions were monitored over time using a digital camera. Body weight changes were recorded 10 d post-infection, and liver, lung, kidney, spleen, and skin tissue samples were collected to evaluate pathological alterations and bacterial loads.

2.16. Statistical analysis

Statistical analysis was performed using GraphPad Prism (v8.0.2). Results are presented as the mean ± SEM. Statistical significance was assessed using one-way ANOVA followed by Dunnett's test. $P < 0.05$ was considered statistically significant.

3. Results and discussion

3.1. Screening of 5,8-dihydroxy-1,4-naphthoquinone and its derivatives for antimicrobial activity

Ten naturally derived 5, 8-dihydroxy-1, 4-naphthoquinone derivatives and 25 naphthoquinone derivatives selected from more than 300 compounds with strong anticancer activity synthesized in our laboratory (Fig. 1 and Table 1) were evaluated against the Gram-negative bacteria *B. subtilis* and *E. coli* and the Gram-positive bacterium *S. aureus* (including MRSA, ATCC 43300). The results of a standard broth K-B test revealed that all 35 compounds lacked antibacterial activity against the two Gram-negative bacteria. However, nine compounds demonstrated antibacterial activity against *S. aureus,* and three compounds, specifically PNP-01, PNP-02, and PNP-08, demonstrated antibacterial activity against MRSA (Tables 2 and 3). The specific antibacterial effects of these compounds against Gram-positive bacteria may be attributed to the structural differences between Gram-positive and Gram-negative bacterial cell surfaces [32].

The MIC and MBC values of the nine shikonin derivatives exhibiting antibacterial activity as well as the established antibiotics penicillin and vancomycin were determined against *S. aureus* and MRSA using the alamarBlue indicator staining method (Table 3). This assay revealed that all compounds showed antimicrobial activity against *S. aureus*, but only PNP-01, PNP-02, and PNP-08 exhibited anti-MRSA activity. However, MRSA cells were resistant to penicillin, PNP-01, and PNP-08 (MIC ≥ 128 μg·mL^{-1}). PNP-02 exhibited an antibacterial effect that was superior to penicillin and only slightly inferior to vancomycin. Additionally, PNP-02 inhibited MRSA with a larger inhibition zone compared to the positive control vancomycin, indicating comparable efficacy against MRSA (Fig. 2A and Table 3).

Time-kill assay was subsequently employed to verify the bactericidal efficacy of PNP-02 against the MRSA strain. The results demonstrated that PNP-02 significantly reduced MRSA growth within 1 h at concentrations of 0.5 × MIC, 1 × MIC, and 2 × MIC. Furthermore, complete inhibition of MRSA growth was observed within 2 h at a concentration of 4 × MIC (Fig. 2B).

3.2. Effect of PNP-02 on the morphology and membrane permeability of MRSA

Biofilms formed by *S. aureus* significantly enhance antibiotic resistance and infection severity [33], thus representing a potential target for novel antimicrobial agents. Antimicrobial compounds may also compromise the bacterial cell wall and cytoplasmic membrane, leading to cell lysis and cytoplasmic content leakage [34]. Here, we used TEM analyses to observe the effects of PNP-02 on the morphology and sub-cellular structures of MRSA cells to investigate the mechanisms of antibacterial activity (Fig. 2C). Control treatment revealed no changes in MRSA morphology or distribution. However, cells treated with 1 × MIC PNP-02 for 2 h exhibited wrinkled and ruptured cell membranes. Moreover, bacteria treated with 2 × MIC PNP-02 lost their spherical shape, displayed decreased and ruptured cell membranes, and expelled cytoplasmic contents. These observations further substantiate the potent bactericidal activity of compound PNP-02 and suggest that it disrupts the MRSA cell membrane.

PI staining was conducted to further evaluate the effects of PNP-02 on the bacterial cell membrane (Fig. 2D). PI typically cannot penetrate intact cell membranes; however, it can enter damaged membranes and bind to DNA, resulting in red fluorescence emission. In the control-treated MRSA, minimal red fluorescence was observed in the PI assay. Conversely, when MRSA was exposed to PNP-02 for 2 h, PI staining resulted in increased cellular red fluorescence. The fluorescence intensity correlated positively with PNP-02 concentration, indicating a dose-dependent effect on membrane permeability. These observations led to the conclusion that PNP-02 compromised the integrity of the bacterial membrane.

A mature bacterial biofilm comprises a community of bacteria encased within a self-produced extracellular polymeric matrix. Numerous chronic bacterial infections are associated with these biofilms, rendering them resistant to conventional antibiotic treatments [35, 36]. The capacity of PNP-02 to impede biofilm formation was evaluated using crystal violet staining. Results indicated that PNP-02 effectively inhibited MRSA biofilm formation (Fig. 2E). Notably, MRSA biofilm formation was significantly suppressed following a 2-hour treatment with PNP-02 at 2 × MIC concentration. However, at concentrations of 0.5 × MIC or below, PNP-02 demonstrated no observable inhibitory effect on biofilm formation.

To further investigate the alteration in cell membrane permeability following PNP-02 treatment, we measured the release of LDH and ALP from the bacteria. LDH leakage from bacteria occurs only when the membrane is compromised, making it a rigorous indicator of cell membrane integrity [37]. This assay revealed

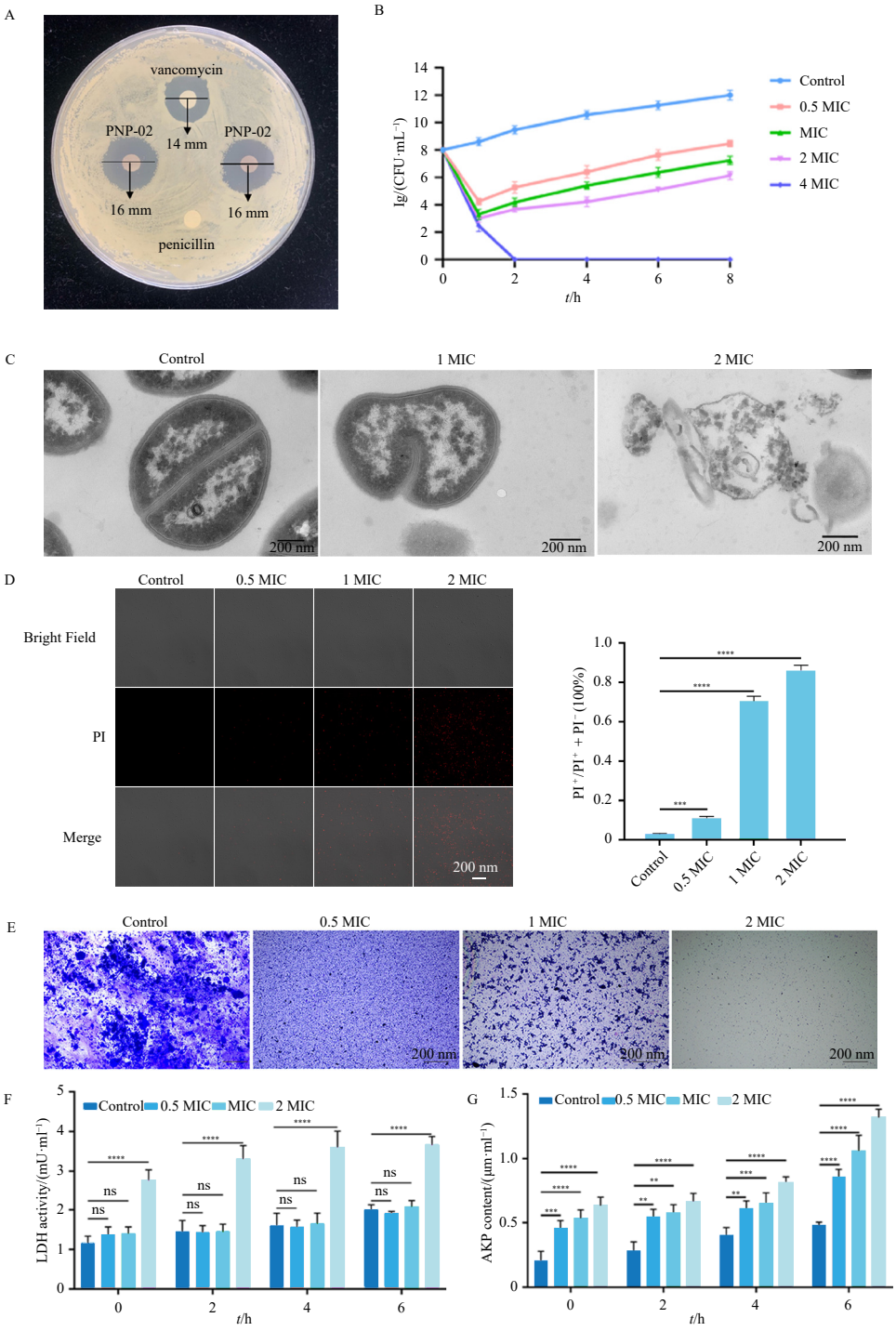

Fig. 2 Inhibitory effect of PNP-02 against MRSA. (A) Drug sensitivity tests of MRSA (ATCC43300) to PNP-02, vancomycin, and penicillin. (B) Time-kill curves of PNP-02 against MRSA. (C) Transmission electron microscopy images of PNP-02-treated MRSA cells. (D) Propidium iodide (PI) staining of PNP-02-treated MRSA cells. (E) MRSA biofilms were treated with PNP-02, stained with crystal violet, and imaged under optical microscopy. The activities of LDH (F) and ALP (G) released to the media from treated with PNP-02 were determined after 0 h, 2 h, 4 h, and 6 h of culture. (n = 3, mean ± SD, $^{***}P < 0.001$, $^{****}P < 0.0001$ *vs* control group).

that PNP-02 indeed damages the bacterial membrane. The increase in LDH activity in the supernatant of MRSA cultures treated with PNP-02 was observed to be both time- and dose-dependent (Fig. 2F).

ALP is located between the cell membrane and cell wall, and its presence outside bacterial cells indicates cell wall damage [38]. In this study, the ALP activity in MRSA culture supernatants exposed to PNP-02 exhibited a time- and dose-dependent response to the compound (Fig. 2G). Collectively, these findings demonstrate that PNP-02 can compromise both the cell wall and cell membrane integrity of MRSA.

3.3. Proteomic analysis of the effect of PNP-02 on MRSA

To elucidate the precise molecular mechanisms underlying the antibacterial effect of PNP-02 against MRSA isolates, we conducted proteomic analyses on untreated and treated cells. These analyses revealed 323 differentially expressed proteins (fold change > 2, false discovery rate < 0.05): 148 proteins exhibited increased levels (red dots), and 175 proteins showed decreased levels (blue dots) in the presence of PNP-02 (Fig. 3A).

To elucidate potential connections between the differentially expressed proteins and genes and antibacterial activity, both GO

and KEGG analyses were performed. The GO analyses specifically examined biological processes, cellular components, and molecular functions. Within the biological processes category, enrichment was observed in proteins related to *de novo* uridine monophosphate (UMP) biosynthesis, cytolysis in other organisms, *de novo* pyrimidine nucleobase biosynthesis, and arginine biosynthesis. Regarding cellular components, enriched proteins were predominantly associated with the extracellular region and plasma membrane. In the molecular functions category, enriched proteins were primarily involved in ATP binding, metal ion binding, and transmembrane transporter activity (Fig. 3B).

KEGG enrichment analysis identified arginine biosynthesis, pyrimidine metabolism, and ABC transporters as the three most significantly enriched pathways (Fig. 3C). Additionally, *S. aureus* infection, and alanine, aspartate, and glutamate metabolism were also prominent among the enriched pathways. Modifications in these pathways may contribute to the antibacterial mechanism of PNP-02. The analysis suggests that arginine biosynthesis and pyrimidine metabolic pathways potentially play crucial roles in the antibacterial mechanisms of PNP-02 against MRSA strains.

The arginine biosynthesis pathway consists of eight different enzymes (encoded by the *argC*, *argJ*, *argB*, *argD*, *argF*, *argR*, *argG*, and *argH* genes), all of which are considered essential for microbial growth in culture. The loss of *argF* directly affects arginine biosynthesis [39]. In this study, the expression of multiple proteins involved in arginine biosynthesis, including ArgF, ArcA, ArcC, ArgG, ArgH, and GudB, were observed to be significantly downregulated following PNP-02 treatment.

The expression levels of genes associated with arginine biosynthesis were further explored with both RT-qPCR and Western blotting assays. The findings revealed a notable decrease in the mRNA levels of *arcA*, *argF*, and *arcC* and the protein level of ArcA, as illustrated in Figs. 3D and 3E, corroborating the findings of the proteomic analysis. These observations suggest that PNP-02 administration may lead to the inhibition of arginine biosynthesis. Moreover, two of the identified genes, *arcA* and *arcC*, are components of the arginine deiminase system, which catalyzes the conversion of L-arginine to L-ornithine, ammonia, and ATP, thus affecting energy production [24].

The pyrimidine synthase pathway is closely associated with the arginine synthetic pathway [29]. These biosynthetic pathways are interconnected through the common metabolite carbamoyl phosphate (CP), which serves as a precursor for both arginine and pyrimidine synthesis (Fig. 3F) [40]. In most Gram-negative bacteria such as *E. coli*, CP is generated by a single enzyme known as carbamoyl phosphate synthase (CPSase), which is encoded by the *carA* and *carB* operons. CPSase synthesizes the high-energy CP required for both pathways from ammonia [40, 41]. It comprises two subunits: a small glutaminase subunit (encoded by *carA*) and a large subunit (encoded by *carB*) [40]. CPSase activity is allosterically regulated by ornithine and inosine monophosphate (IMP) as activators and UMP as an inhibitor. Ornithine activation of CPSase is crucial for promoting the ornithine transcarbamylase (*argF*) reaction by increasing CP levels for arginine synthesis. The contrasting effects of UMP and IMP on CPSase activity help maintain the balance between purine and pyrimidine synthesis necessary for biomass production [40]. The complex regulation of CPSase activity by ornithine and UMP, along with the interaction between the carbamylating enzymes argF and pyrB in arginine and UMP biosynthesis, helps maintain the equilibrium between CP production and consumption. This balance is essential for meeting the metabolic demands of both pathways, as depicted in Fig. 3F [40].

The biosynthesis of pyrimidine nucleotides can impact biofilm formation by modulating the expression of several genes, including *csgD*, *csgE*, and *csgF* [42], which encode proteins that assemble into extracellular fibers enhancing biofilm integrity. The initial step in *de novo* pyrimidine nucleotide synthesis involves the production of uracil nucleotides as UMP. This study revealed that the expression levels of multiple genes involved in pyrimidine biosynthesis, including *carA*, *carB*, *pyrB, pyrC, pyrD*, *pyrE*, and *pyrF*, were significantly decreased after PNP-02 treatment. PyrB and CarB are essential enzymes in the nucleotide salvage pathway [43]. Our research demonstrated that PNP-02 treatment inhibited the expression of these two genes, and the levels of six other genes involved in producing the raw material for UMP synthesis decreased markedly, suggesting that PNP-02 impeded the salvage of pyrimidine nucleotides. The results of our RT-qPCR and Western blot analyses of genes and proteins related to pyrimidine synthesis corroborated our proteomic findings, demonstrating that the mRNA levels of *carB*, *pyrB*, and *pyrF* and the protein level of pyrF were significantly reduced upon PNP-02 treatment (Figs. 3D and 3E).

The crucial role of UMP in regulating biofilm formation and providing feedback inhibition of pyrimidine synthesis [44] suggests that inhibiting UMP synthesis, and consequently nucleic acid synthesis, may be the primary mechanism underlying the bactericidal effect of naphthoquinone. The proteins CarA, CarB, PyrB, and PyrC are located on one polypeptide chain, while PyrE and PyrF are on another, indicating that the genes encoding these proteins might constitute an operon. Based on this, we hypothesized that PNP-02 could potentially inhibit MRSA biofilm formation by interfering with pyrimidine metabolism. However, this hypothesis requires further investigation to be conclusively established.

3.4. PNP-02 promotes skin wound healing in a mouse model of MRSA infection

The study aimed to evaluate the bactericidal effects and therapeutic efficacy of PNP-02 on skin wounds using a mouse model of skin MRSA infection (Fig. 4A). Skin wounds were induced in 25 mice, and the mice were then randomly divided into five groups. One group (control) was allowed to heal normally, but the wounds in the other mice were inoculated with MRSA. One group of MRSA-treated mice was left untreated (model control), and the other mice were treated by smear with 0.5 ×, 1 ×, or 2 × MIC PNP-02. Each mouse was monitored every two days for changes in skin appearance, and photographs of the infected wounds were captured at various time points post-surgery (Fig. 4B). Interestingly, while the model control mice exhibited symptoms of bacterial ulcers and sepsis, the groups treated with 0.5 ×, 1 ×, or 2 × MIC PNP-02 did not exhibit these symptoms during the healing process. Notably, the group treated with 2 × MIC PNP-02 showed accelerated healing compared to the groups treated with lower concentrations of PNP-02. Fig. 4C visually depicts the changes in wound length over time for each treatment group. These findings suggest that PNP-02 exhibits potent bactericidal activity on skin wounds, with higher concentrations enhancing therapeutic efficacy and accelerating wound healing.

Mouse skin samples were collected, homogenized, and plated on agar plates to quantify bacterial colonies post-treatment. The tissues treated with 2 × MIC PNP-02 led to the growth of few colonies, indicating strong antibacterial activity (Fig. 4D). Histopathological examination revealed reduced wound sizes and attenuated inflammatory responses in the 2 × MIC PNP-02 group relative to the model control group, further corroborating PNP-02's effectiveness *in vivo* (Fig. 4E). The consistent body weights of mice throughout the study and the absence of detectable damage or toxicity in major organs post-PNP-02 treatment indicate the biocompatibility and safety of PNP-02 as an antibacterial agent for cutaneous wound infections in clinical applications (Figs. 4F

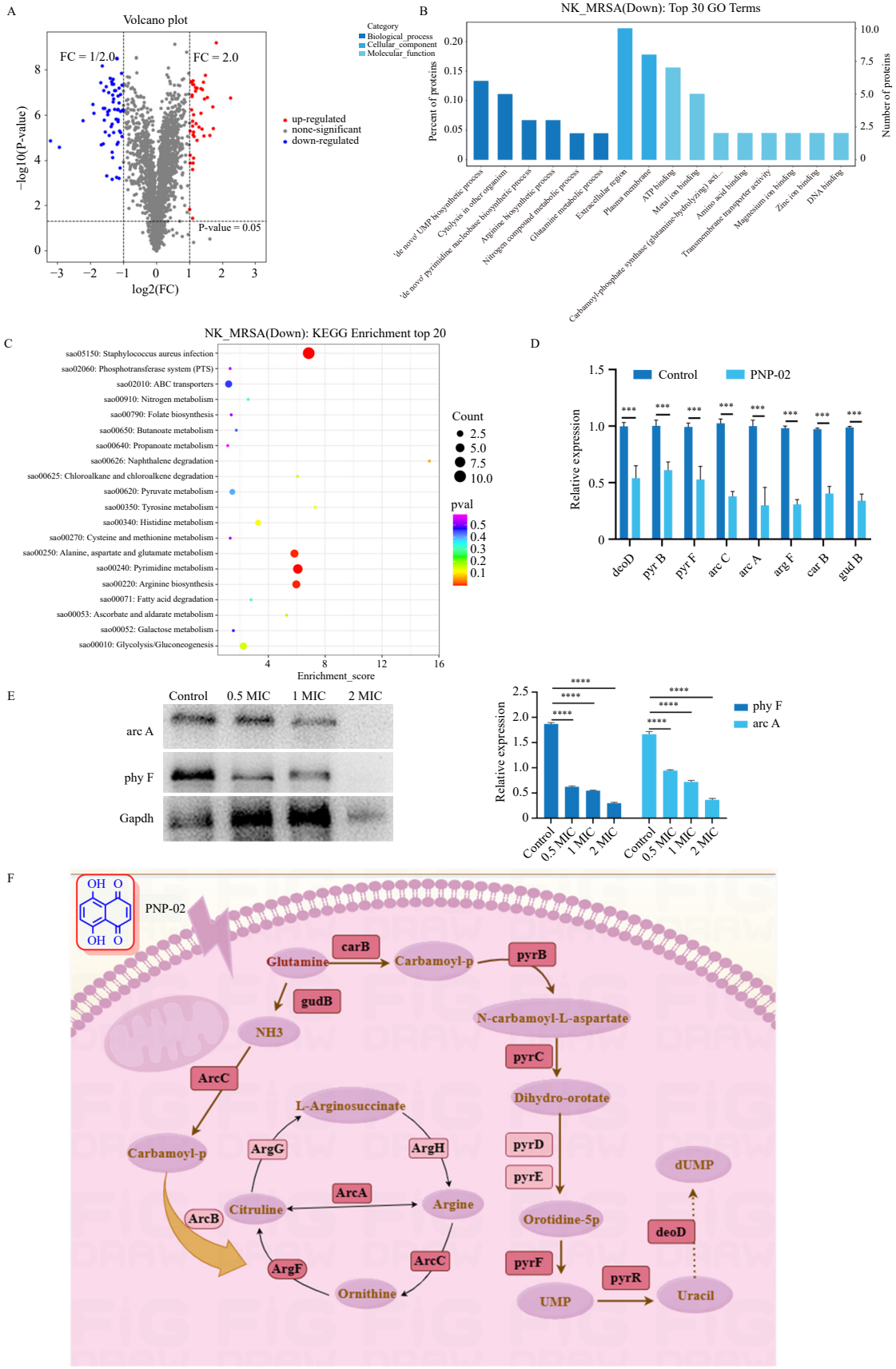

Fig. 3 Proteomic analysis of changes to MRSA upon treatment with PNP-02. (A) Volcano plot of differentially expressed proteins upon PNP-02 treatment. (B, C) Pathway analyses of DEGs using the GO (B) and KEGG (C) methods. (D) The relative expression levels of *deoD*, *pyrB*, *pyrF*, *arcC*, *arcA*, *argF*, and *gudB* in PNP-02-treated MRSA were determined by RT-qPCR; the levels were normalized to the expression of 16S RNA. (E) Western blotting analyses of the expressions of PhyF and ArcA in control or PNP-02-treated MRSA. Band intensities (left) were quantified using ImageJ and normalized to GAPDH (right). (F) Diagram showing the proposed antibacterial mechanism of PNP-02. Red box: Downregulated genes have been verified by qPCR. ($^{*}P < 0.05$, $^{**}P < 0.01$, $^{***}P < 0.001$ *vs* control group).

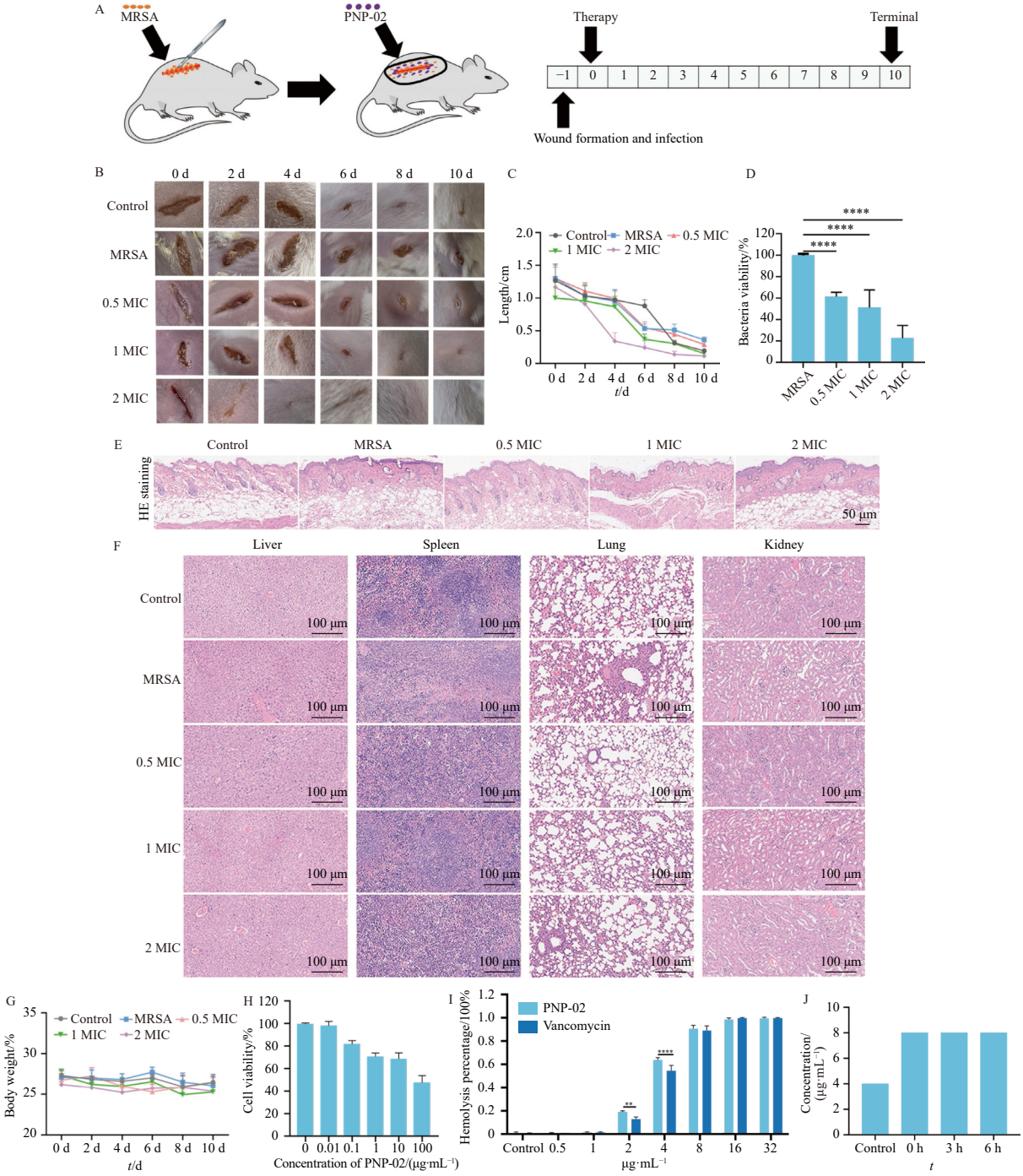

Fig. 4 PNP-02 improves skin healing in a mouse skin wound infection model. (A) Schematic depiction of the procedure. (B) Representative photographs of infected skin. (C) The length of the infected skin of mice from each treatment group over time. (D) The body weights of the mice were determined. (E) Histological evaluation of liver, spleen, lung, and kidney tissues. (F) Images of hematoxylin and eosin-stained skin tissue sections from each treatment group 10 d after wounding. Scale bar = 50 μm. (G) The number of surviving bacteria was determined as CFU at the end of the experiment. (H) Cell viability of LO2 cells treated with the indicated concentrations of PNP-02 for 24 h. (I) Hemolysis in the presence of different concentrations of PNP-02. (J) MBC values of PNP-02 against MRSA after 0 h, 3 h, and 6 h incubation in 50% plasma. (n = 5, mean ± SD, NS: not significant; $^{*}P < 0.05$, $^{****}P < 0.0001$ *vs* control group)

and G). These promising *in vivo* results highlight the potential of PNP-02 as a viable treatment option for bacterial infections.

3.5. Evaluation of the biocompatibility and stability of PNP-02 in vitro

The CCK-8 assay was utilized to evaluate the cytotoxic effect of PNP-02 on human LO2 cells. When cells were exposed to 100 μg·mL^{-1} PNP-02 for 24 h, cell survival rates exceeded 60%. This finding indicates that PNP-02 exhibits minimal toxicity toward host cells, suggesting its safety for use at concentrations beyond the effective dose (Fig. 4H). Furthermore, PNP-02 demonstrated excellent biocompatibility under physiological conditions in hemolysis assays. Incubation of red blood cells with PNP-02 at 1 × MIC resulted in no observable cell rupture, confirming the compound's non-hemolytic nature and overall safety as an antimicrobial agent (Fig. 4I). Plasma stability is crucial for drug efficacy due to the potential impact of plasma hydrolases on bioavailability. Notably, PNP-02's MBC value remained stable even after 6 h in plasma, indicating consistent antibacterial activity and robust plasma stability (Fig. 4J). These results suggest that PNP-02 effectively resists plasma hydrolase degradation, maintaining its antimicrobial efficacy. Moreover, its safety profile and biocom-

patibility under specific conditions position PNP-02 as a promising candidate for antimicrobial applications.

4. Conclusion

This study demonstrates that PNP-02 exhibits potent bactericidal activity against *S. aureus* and MRSA. Notably, the efficacy of PNP-02 is concentration-dependent, revealing a strong, dose-dependent bactericidal effect, a crucial factor to consider when developing appropriate dosing strategies for potential therapeutic applications. Mechanistically, PNP-02 induces bacterial cell death by compromising cell membrane integrity, associated with disrupting key biochemical pathways such as arginine biosynthesis and pyrimidine metabolism. This elucidation of PNP-02's mechanisms not only clarifies its mode of action but also suggests additional metabolic vulnerabilities in Gram-positive bacteria, potentially identifying new antibacterial targets. The significance of this research extends beyond explicating PNP-02's mechanism, as it establishes a foundation for its future clinical application. Consequently, PNP-02 emerges as a promising candidate for the development of novel antimicrobial therapies, underscoring its potential to address challenges posed by antibiotic resistance.

Ethical approval

The study was approved by the Animal Welfare Ethics Committee of the Jiangsu Huachuang Sino Pharma Tech Co., Ltd. (No. SY23033-P001-01)

Funding

This study was financially supported by the National Natural Science Foundation of China (Nos. U1903201, 21702100, 21907051), the Program for Changjiang Scholars and Innovative Research Team in University (No. IRT_14R27), the Natural Science Foundation of Jiangsu Bureau of Science and Technology (No. BK20191254), and the Fundamental Research Funds for Central Universities (No. 020814380151).

Declaration of competing interest

The authors declare no conflicts of interest regarding the publication of this paper.

Acknowledgments

The authors thank for the help of Biorender.com in the production and modification of the figures in the article (https://app.biorender.com).

References

1 Misic AM, Davis MF, Tyldsley AS, et al. The shared microbiota of humans and companion animals as evaluated from carriage sites. *Microbiome*. 2015;3:2. https://doi.org/10.1186/s40168-014-0052-7.
2 Murra M, Mortensen KL, Wang M. Livestock-associated methicillin-resistant (clonal complex 398) causing bacteremia and epidural abscess. *Int J Infect Dis*. 2019;81:107-109. https://doi.org/10.1016/j.ijid.2019.01.012.
3 Service RF. Antibiotics that resist resistance. *Science*. 1995;270(5237):724-727. https://doi.org/10.1126/science.270.5237.724.
4 Collin SM, Shetty N, Guy R, et al. Group B *Streptococcus* in surgical site and non-invasive bacterial infections worldwide: A systematic review and meta-analysis. *Int J Infect Dis*. 2019;83:116-129. https://doi.org/10.1016/j.ijid.2019.04.017.
5 Huai W, Ma QB, Zheng JJ, et al. Distribution and drug resistance of pathogenic bacteria in emergency patients. *World J Clin Cases*. 2019;7(20):3175-3184. https://doi.org/10.12998/wjcc.v7.i20.3175.
6 Chen CH, Chen L, Mao CY, et al. Natural extracts for antibacterial applications. *Small*. 2024;20(9):e2306553. https://doi.org/10.1002/smll.202306553.
7 Cho SY, Chung DR. Infection prevention strategy in hospitals in the era of community-associated methicillin-resistant *Staphylococcus Aureus* in the Asia-Pacific region: a review. *Clin infec dis*. 2017;64(suppl_2):S82-S90. https://doi.org/10.1093/cid/cix133.
8 Duvauchelle V, Majdi C, Benimelis D, et al. Synthesis, structure elucidation, antibacterial activities, and synergistic effects of novel Juglone and Naphthazarin derivatives against clinical methicillin-resistant *Staphylococcus aureus* strains. *Front Chem*. 2021;9:773981. https://doi.org/10.3389/fchem.2021.773981.
9 da Silva FD, Ferreira VF. Natural naphthoquinones with great importance in medicinal chemistry. *Curr Org Synth*. 2016;13(3):334-371. https://doi.org/10.2174/1570179412666150817220343.
10 Aminin D, Polonik S. 1, 4-naphthoquinones: some biological properties and application. *Chem Pharm Bull*. 2020;68(1):46-57. https://doi.org/10.1248/cpb.c19-00911.
11 Prati F, Bergamini C, Molina MT, et al. 2-Phenoxy-1, 4-naphthoquinones: from a multitarget antitrypanosomal to a potential antitumor profile. *J Med Chem*. 2015;58(16):6422-6434. https://doi.org/10.1021/acs.jmedchem.5b00748.
12 Paul P, Chakraborty P, Chatterjee A, et al. 1, 4-Naphthoquinone accumulates reactive oxygen species in *Staphylococcus aureus*: a promising approach towards effective management of biofilm threat. *Arch Microbiol*. 2021;203(3):1183-1193. https://doi.org/10.1007/s00203-020-02117-1.
13 Tomozane H, Takeuchi Y, Choshi T, et al. Syntheses and antifungal activities of dl-griseofulvin and its congeners. I. *Chem Pharm Bull*. 1990;38(4):925-929. https://doi.org/10.1248/cpb.38.925.
14 Topçu S, Seker MG. *In vitro* antimicrobial effects and inactivation mechanisms of 5, 8-dihydroxy-1, 4-napthoquinone. *Antibiotics-Basel*. 2022;11(11):1537. https://doi.org/10.3390/antibiotics11111537.
15 Meem MH, Yusuf SB, Al Abbad SS, et al. Exploring the anticancer and antibacterial potential of naphthoquinone derivatives: a comprehensive computational investigation. *Front Chem*. 2024;12:1351669. https://doi.org/10.3389/fchem.2024.1351669.
16 Auber RP, Suttiyut T, McCoy RM, et al. Hybrid de novo genome assembly of red gromwell (*Lithospermum erythrorhizon*) reveals evolutionary insight into shikonin biosynthesis. *Hortic Res-England*. 2020;7(1):82. https://doi.org/10.1038/s41438-020-0301-9.
17 Li QQ, Chae HS, Kang OH, et al. Synergistic antibacterial activity with conventional antibiotics and mechanism of action of shikonin against methicillin-resistant *Staphylococcus Aureus*. *Int J Mol Sci*. 2022;23(14):1551. https://doi.org/10.3390/ijms23147551.
18 Farzi S, Rezazadeh M, Mirhosseini A, et al. Genetic diversity of healthcare-associated methicillin-resistant *Staphylococcus Aureus* isolates from Southern Iran. *Acta Microbiol Imm H*. 2021;68(2):121-127. https://doi.org/10.1556/030.2021.01365.
19 Pani A, Lucini V, Dugnani S, et al. Erdosteine enhances antibiotic activity against bacteria within biofilm. *Int J Antimicrob Ag*. 2022;59(3):106529. https://doi.org/10.1016/j.ijantimicag.2022.106529.
20 Yuan Z, Wang J, Qu Q, et al. Celastrol combats methicillin-resistant *Staphylococcus Aureus* by targeting delta(1) -pyrroline-5-carboxylate dehydrogenase. *Adv Sci*. 2023;10(25):e2302459. https://doi.org/10.1002/advs.202302459.
21 Dubee V, Chau F, Arthur M, et al. The *in vitro* contribution of autolysins to bacterial killing elicited by amoxicillin increases with inoculum size in *Enterococcus faecalis*. *Antimicrob Agents Chemother*. 2011;55(2):910-912. https://doi.org/10.1128/AAC.01230-10.
22 Zhang S, Tang H, Wang Y, et al. Antibacterial and antibiofilm effects of flufenamic acid against methicillin-resistant *Staphylococcus Aureus*. *Pharmacol Res*. 2020;160:105067. https://doi.org/10.1016/j.phrs.2020.105067.
23 Yuan WQ, Yuk HG. Antimicrobial efficacy of plant extract against and methicillin-resistant and its application potential with cooked chicken. *Food Microbiol*. 2018;72:176-184. https://doi.org/10.1016/j.fm.2017.12.002.
24 Liu B, Yang Y, Wu H, et al. Zeolitic imidazolate framework-8 triggers the inhibition of arginine biosynthesis to combat methicillin-resistant *Staphylococcus Aureus*. *Small*. 2023;19(14):e2205682. https://doi.org/10.1002/smll.202205682.
25 Shu G, Xu D, Zhang W, et al. Preparation of shikonin liposome and evaluation of its *in vitro* antibacterial and *in vivo* infected wound healing activity. *Phytomedicine*. 2022;99:154035. https://doi.org/10.1016/j.phymed.2022.154035.
26 Duan JJ, Li ML, Hao ZH, et al. Subinhibitory concentrations of resveratrol reduce alpha-hemolysin production in *Staphylococcus Aureus* isolates by downregulating saeRS. *Emerg Microbes Infec*. 2018;7(1):136. https://doi.org/10.1038/s41426-018-0142-x.
27 Xu T, Yan XT, Kang AY, et al. Development of membrane-targeting fluorescent 2-phenyl-1 H-phenanthro[9, 10-d]imidazole-antimicrobial peptide mimic conjugates against methicillin-resistant *Staphylococcus aureus*. *J Med Chem*. 2024;67(11):9302-9317. https://doi.org/10.1021/acs.jmedchem.4c00436.
28 Liu W, Wang X, Liu Y, et al. Effects of early florfenicol exposure on glutathione signaling pathway and PPAR signaling pathway in chick liver. *Ecotoxicol Environ Saf*. 2022;237:113529. https://doi.org/10.1016/j.ecoenv.2022.113529.
29 Simitsopoulou M, Kadiltzoglou P, Antachopoulos C, et al. Daptomycin exerts differential immunomodulatory effects on host responses against methicillin-resistant biofilms. *Int J Antimicrob Ag*. 2022;60(4):106666. https://doi.org/10.1016/j.ijantimicag.2022.106666.
30 O'Reilly EB, Johnson MD, Rohrich RJ. Comprehensive review of methicillin-resistant *Staphylococcus Aureus*: screening and preventive recommendations for plastic surgeons and other surgical health care providers. *Plast Reconstr Surg*. 2014;134(5):1078-1089. https://doi.org/10.1097/PRS.0000000000000626.
31 Ma YD, Lai XH, Wen ZL, et al. Design, synthesis and biological evaluation of novel modified dual-target shikonin derivatives for colorectal cancer treatment. *Bioorg Chem*. 2023;139:106703. https://doi.org/10.1016/j.bioorg.2023.106703.

32 Zhang XM, Qin M, Xu MJ, et al. The fabrication of antibacterial hydrogels for wound healing. *Eur Polym J*. 2021;146:110268. https://doi.org/10.1016/j.eurpolymj.2021.110268.
33 Patra JK, Das G, Baek KH, et al. Antibacterial mechanism of the action of Enteromorpha linza *L. essential* oil against *Escherichia coli* and *Salmonella Typhimurium*. *Bot Stud*. 2015;56(1):13. https://doi.org/10.1186/s40529-015-0093-7.
34 Gangwar B, Kumar S, Darokar MP, et al. Glabridin averts biofilms formation in methicillin-resistant *Staphylococcus Aureus* by modulation of the surfaceome. *Front Microbiol*. 2020;11:1779. https://doi.org/10.3389/fmicb.2020.01779.
35 Zeng Q, Wang ZJ, Chen S, et al. Phytochemical and anti-MRSA constituents of Zanthoxylum nitidum. *Biomed Pharmacother*. 2022;148:112758. https://doi.org/10.1016/j.biopha.2022.112758.
36 Taraszkiewicz A, Fila G, Grinholc M, et al. Innovative strategies to overcome biofilm resistance. *BioMed Res Int*. 2013;2013:150653. https://doi.org/10.1155/2013/150653.
37 Zhang WP, Chen LH, Feng H, et al. Rifampicin-induced injury in HepG2 cells is alleviated by TUDCA *via* increasing bile acid transporters expression and enhancing the Nrf2-mediated adaptive response. *Free Radical Biology and Medicine*. 2017;112: 24–35. https://doi.org/10.1016/j.freeradbiomed.2017.07.003.
38 Lin YL, Tang X, Xu LZ, et al. Antibacterial properties and possible action mechanism of chelating peptides-zinc nanocomposite against *Escherichia coli*. *Food Control*. 2019;106:106675. https://doi.org/10.1016/j.foodcont.2019.06.001.
39 DeJesus MA, Gerrick ER, Xu WZ, et al. Comprehensive essentiality analysis of the mycobacterium tuberculosis genome *via* saturating transposon mutagenesis. *mBio*. 2017;8(1):e02133-16. https://doi.org/10.1128/mBio.02133-16.
40 Charlier D, Minh PNL, Roovers M. Arginine biosynthesis in *Escherichia coli*: experimental perturbation and mathematical modeling. *Amino Acids*. 2018;50(12):1647-1661. https://doi.org/10.1007/s00726-018-2654-z.
41 Caldara M, Dupont G, Leroy F, et al. Arginine biosynthesis in *Escherichia coli*: experimental perturbation and mathematical modeling. *J Biol Chem*. 2008;283(10):6347-6358. https://doi.org/10.1074/jbc.M705884200.
42 Garavaglia M, Rossi E, Landini P. The pyrimidine nucleotide biosynthetic pathway modulates production of biofilm determinants in *Escherichia coli*. *Plos One*. 2012;7(2):e31252. https://doi.org/10.1371/journal.pone.0031252.
43 Cheng F, Mo YA, Chen KY, et al. Integration of metabolomics and transcriptomics indicates changes in MRSA exposed to terpinen-4-ol. *Bmc Microbiol*. 2021;21(1):305. https://doi.org/10.1186/s12866-021-02348-2.
44 Karaolis DKR, Rashid MH, Chythanya R, et al. c-di-GMP (3′-5′-cyclic diguanylic acid) inhibits cell-cell interactions and biofilm formation. *Antimicrob Agents Ch*. 2005;49(3):1029-1038. https://doi.org/10.1128/AAC.49.3.1029-1038.2005.